PAPER

Observation of subcritical geodesic acoustic mode excitation in the large helical device

IOP Publishing | International Atomic Energy Agency Nuclear Fusion

Nucl. Fusion **57** (2017) 072009 (9pp) https://doi.org/10.1088/1741-4326/aa665a

Observation of subcritical geodesic acoustic mode excitation in the large helical device

T. Ido[1], K. Itoh[1,2], M. Lesur[3], M. Osakabe[1,4], A. Shimizu[1], K. Ogawa[1,4], M. Nishiura[5], I. Yamada[1], R. Yasuhara[1], Y. Kosuga[2], M. Sasaki[2], K. Ida[1,2], S. Inagaki[2], S.-I. Itoh[2] and the LHD Experiment Group[1]

[1] National Institute for Fusion Science, National Institutes of Natural Sciences, 322-6 Oroshi, Toki, Gifu 509-5292, Japan
[2] Research Institute for Applied Mechanics, Kyushu University, 6-1 Kasuga-koen, Kasuga, Fukuoka 816-8580, Japan
[3] Institut Jean Lamour, UMR 7198 CNRS—Université de Lorraine, Campus Sciences, Bd des Aiguillettes, BP 70239, 54 506 VANDOEUVRE-LES-NANCY Cedex, France
[4] SOKENDAI (Graduate University for Advanced Study), 322-6 Oroshi, Toki, Gifu 509-5292, Japan
[5] Graduate School of Frontier Sciences, University of Tokyo, 5-1-5 Kashiwanohara, Kashiwa, Chiba 277-8561, Japan

E-mail: ido@LHD.nifs.ac.jp

Received 15 September 2016, revised 27 February 2017
Accepted for publication 13 March 2017
Published 19 April 2017

Abstract

The abrupt and strong excitation of the geodesic acoustic mode (GAM) has been found in the large helical device (LHD), when the frequency of a chirping energetic particle-driven GAM (EGAM) approaches twice that of the GAM frequency. The temporal evolution of the phase relation between the abrupt GAM and the chirping EGAM is common in all events. The result indicates a coupling between the GAM and the EGAM. In addition, the nonlinear evolution of the growth rate of the GAM is observed, and there is a threshold in the amplitude of the GAM for the appearance of nonlinear behavior. A threshold in the amplitude of the EGAM for the abrupt excitation of the GAM is also observed. According to one theory (Lesur *et al* 2016 *Phys. Rev. Lett.* **116** 015003, Itoh *et al* 2016 *Plasma Phys. Rep.* **42** 418) the observed abrupt phenomenon can be interpreted as the excitation of the subcritical instability of the GAM. The excitation of a subcritical instability requires a trigger and a seed with sufficient amplitude. The observed threshold in the amplitude of the GAM seems to correspond with the threshold in the seed, and the threshold in the amplitude of the EGAM seems to correspond with the threshold in the magnitude of the trigger. Thus, the observed threshold supports the interpretation that the abrupt phenomenon is the excitation of a subcritical instability of the GAM.

Keywords: GAM, EGAM, subcritical instability, abrupt excitation, energetic particle

(Some figures may appear in colour only in the online journal)

1. Introduction

Understanding particle and heat transport in magnetized plasmas is an important issue for designing nuclear fusion reactors with sufficient predictability. Since the transport is caused dominantly by fluctuations, understanding the properties of these fluctuations, especially the excitation conditions and the saturation level, is essential for assessing the performance of plasmas.

Linear analysis of the excitation condition of instabilities provides a guide for the production of laboratory plasmas. However, the prediction of the onset of instabilities is an open question, as reviewed in [1]. In particular, there is room to improve the understanding of the sudden increase in the growth

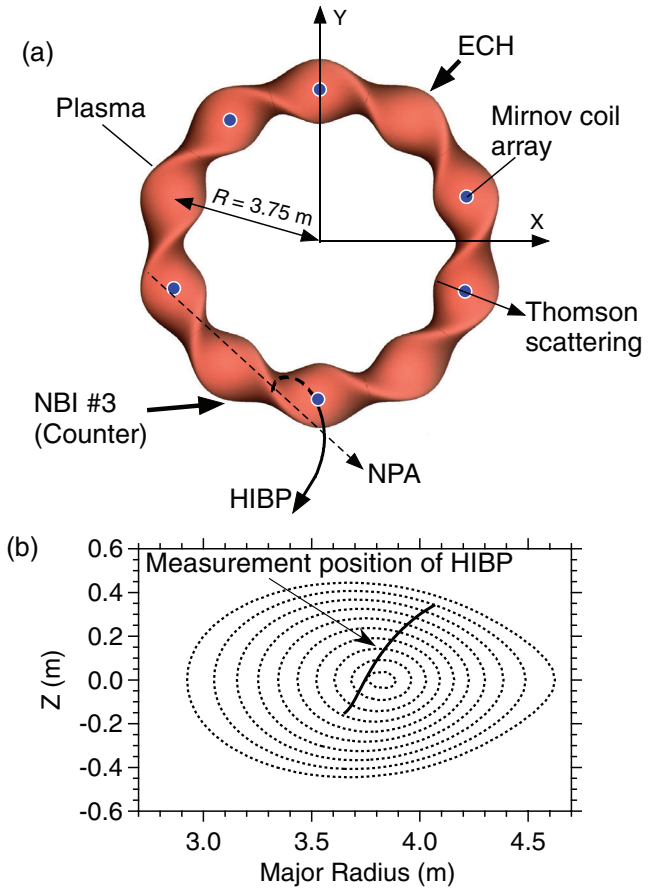

Figure 1. (*a*) A top view of the LHD plasma and the layout of the heating and diagnostic equipment. (*b*) The measurement location of the HIBP during a sweep of the probe beam. The nested dotted contours are the poloidal cross sections of the magnetic surfaces calculated by the VMEC code (Hirshman *et al* [40]).

rate of instabilities, which is featured in abrupt phenomena such as sawtooth oscillation, or disruption in current-carrying toroidal plasmas and solar flares. The rate of change of the linear growth rate is limited by the rate of change of the global equilibrium parameters, which is too slow to explain the abrupt onset. This difficulty is known as the trigger problem, and has been a challenge in laboratory plasmas and astro-plasmas for more than a couple of decades [1, 2]. One of the working hypotheses for understanding the trigger problem is that of subcritical instability, which is driven nonlinearly in the linearly stable parameter region, if the initial seed is large enough. In magnetically confined plasmas, theoretical works have predicted several subcritical instabilities: current-diffusive interchange turbulence [3], magnetic island formation due to the neoclassical tearing mode [4], and instabilities caused by kinetic nonlinearity, including those of the fast ion-driven instabilities [5–12]. So far, however, there has been no clear experimental result demonstrating the subcritical instabilities in plasmas.

Recently, the abrupt excitation of the geodesic acoustic mode (GAM) [13] has been found in magnetically confined toroidal plasmas in the large helical device (LHD) [14]. This occurs in the presence of an energetic particle-driven GAM (EGAM) [15] with nonlinear temporal evolution of the frequency. EGAMs have been widely observed in toroidal plasmas such as JET [16, 17], DIII-D [18], LHD [19, 20], JT-60U [21], ASDEX-Upgrade [22] and HL-2A [23]. The frequency of the EGAM often chirps up quickly, and the timescale (~several ms) is much faster than the timescale of change in the global equilibrium parameters. The evolution corresponds with the evolution of structures in the velocity space of the energetic particle described by the Berk–Briezman model [24]. However, the timescale of the abrupt phenomenon observed in this study is much faster than that of the EGAM, and the amplitude is larger than the variation in the amplitude of the EGAM. These observations suggest the importance of a different excitation mechanism from the ordinary EGAM. In previous work [14], it has been shown that the observed behavior of an abrupt GAM is consistent with the features of its subcritical instability, as predicted by a theoretical model proposed in [25–27]. The onset of subcritical instability requires a seed perturbation with sufficient amplitude, and the observed threshold in the amplitude of the abrupt GAM seems to correspond with the magnitude of the seed. As for the seed trigger, however, only the reproducibility of the Lissajous diagram between the GAM and the EGAM has suggested a trigger by the latter. This study aims at a deeper understanding of the excitation mechanism of the abrupt phenomenon. In particular, the role of the EGAM is described by presenting the amplitude relation between the GAM and the EGAM as well as the phase relation.

The paper is organized as follows. In section 2, the apparatus is described. The experimental results are presented in section 3. The measured temporal evolution of the abrupt excitation phenomenon and the analysis of the phase and amplitude relations between the abrupt GAM and the EGAM will be presented. The results reveal the role of the EGAM for the abrupt excitation of the GAM, and these results are summarized in section 4.

2. Apparatus

The LHD is a superconducting heliotron device with a major radius of 3.9 m and an average minor radius of 0.65 m [28]. In this experiment, the produced plasmas have a major radius of 3.75 m and an average minor radius (a_{99}) of approximately 0.6 m, where the average minor radius is defined as the radius of a magnetic surface in which 99% of the stored energy is included. The top view of the plasma is shown in figure 1(*a*). The experiment was performed under a magnetic field strength of 1.375 T. The fuel gas is hydrogen, and the plasma was produced and sustained by a neutral hydrogen beam injection (NBI) in the counter direction with an energy of 175 keV, where 'counter direction' means that the plasma current driven by the injected beam decreases the original rotational transform of the magnetic field line. The power of the neutral beam ionized in the plasma is about 140 kW. For strong excitation of the energetic particle-driven instability, a positive gradient in the high energy (supra-thermal) range of the velocity space of ions is required. Thus, in order to increase the slowing-down time of the injected beam, the electron temperature is increased by superposing electron cyclotron heating (ECH) with a power of 2.5 MW.

For measuring the toroidal mode structure of the magnetic field fluctuations ($\widetilde{B}_{\mathrm{p}}$), six Mirnov coils are installed on

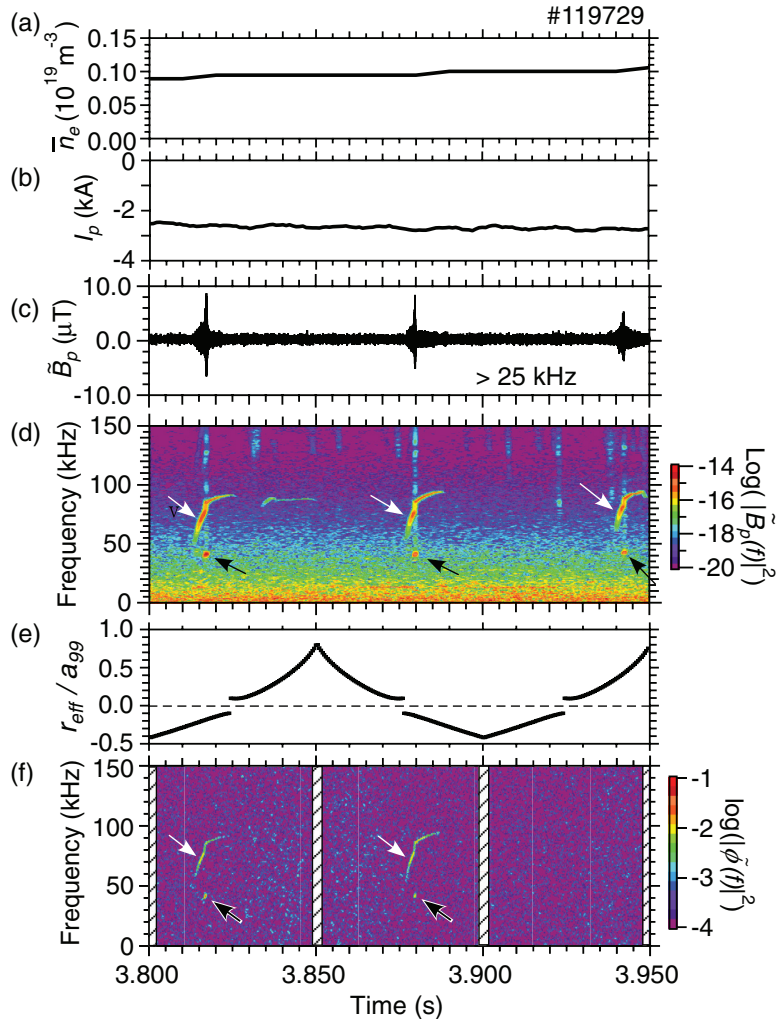

Figure 2. (*a*) The line-averaged electron density, (*b*) the plasma current, (*c*) the magnetic field fluctuations measured by a Mirnov coil, and (*d*) its spectrogram. (*e*) The measurement location of the HIBP, where $r_{\rm eff}$ is the average minor radius, and a_{99} is the average minor radius of a magnetic flux surface which includes 99% of the stored energy. (*f*) A spectrogram of the electric field fluctuation measured by the HIBP; the white and black arrows indicate the EGAM and the abruptly excited GAM, respectively.

the vacuum vessel of the LHD at distant toroidal locations, as shown in figure 1(*a*). The radial profiles of the electric potential fluctuation ($\widetilde{\phi}$) and the density fluctuation ($\tilde{n}$) are measured by a heavy ion beam probe (HIBP), and the measurement location moves along a curve shown in figure 1(*b*) by changing the injection angle of the probe beam at a frequency of 10 Hz [29, 30]. Thus, the electric potential can be measured at the normalized minor radius from −0.3 to 0.6, where minus (plus) refers to the lower (upper) equatorial plane of the torus. In order to measure the energy spectrum of the confined ions, a neutral particle analyzer (NPA) is installed [31].

3. Experimental results

3.1. Experimental condition and typical temporal evolution

The typical waveforms of a discharge are shown in figure 2. The line-averaged electron density is approximately 0.1×10^{19} ($\rm m^{-3}$) (figure 2(*a*)), the central electron temperature is approximately 8 ± 3 keV, and the slowing-down time of the injected beam ion (H^+) is approximately 20 s. As a result, the energy spectrum of the confined ions has a steep positive gradient below the energy of the NBI [32, 33]. The temperature of the bulk ion is approximately 0.4 keV [32]. The plasma current induced by the counter NBI is lower than 3 kA, which is not sufficient to change the monotonic magnetic shear.

The poloidal magnetic field fluctuations ($\widetilde{B}_{\rm p}$) measured by a Mirnov coil, and its spectrogram, are shown in figures 2(*c*) and (*d*), respectively. Figures 2(*e*) and (*f*) show the measurement location of the HIBP and a spectrogram of the electric potential fluctuations measured by it. Coherent modes with frequency up-chirping, which corresponds with the evolution in the velocity space distribution function [24], from about 50 kHz to 90 kHz appear intermittently, as shown by white arrows in both $\widetilde{B}_{\rm p}$ (figure 2(*d*)) and $\widetilde{\phi}$ (figure 2(*f*)). These have been identified as EGAMs [33], and this mode is referred to as 'EGAM' in the latter part of this paper. The EGAMs are only observed in low-density plasmas ($<0.3 \times 10^{19}(\rm m^{-3})$) in which the energetic particles do not slow down sufficiently, as shown in [33].

When the frequency of the EGAM approaches 80 kHz, another mode with half the frequency of the EGAM is

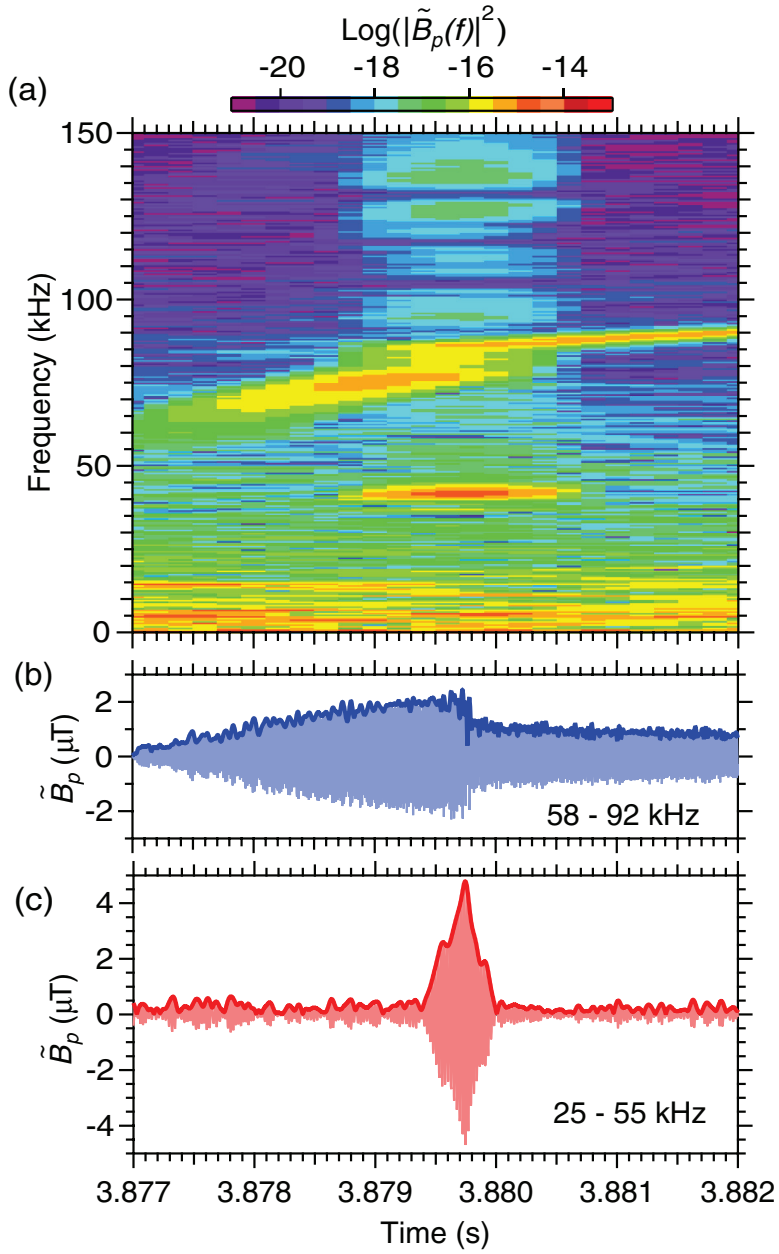

Figure 3. (*a*) A spectrogram of the magnetic field fluctuations ($\widetilde{B}_{\rm p}$). (*b*) and (*c*) Show the waveforms extracted by using numerical band-pass filters with a pass band of 58–92 kHz and 25–55 kHz, respectively; (*b*) corresponds with the EGAM and (*c*) corresponds with the abruptly excited mode. Bold curves show the envelopes.

abruptly and transiently excited, as marked by black arrows in figures 2(*d*) and (*f*). An expanded view of $\widetilde{B}_{\rm p}$ is shown in figure 3. The duration time of the abruptly excited mode with the frequency of 41.5 kHz is less than a millisecond, and this is much shorter than the duration of the EGAM (~10 ms). The GAM frequency [34] calculated with the parameters of the bulk plasma, when assumed to be pure hydrogen plasma, is 56 ± 10 kHz. Although the frequency of 41.5 kHz is smaller than the calculated GAM frequency, the difference can be explained by the effect of energetic particles [15, 33, 35] and of impurity ions. The abruptly excited mode at 41.5 kHz has been identified as a GAM because the frequency and the spatial structures of the electric potential fluctuation and the density fluctuation associated with the mode agree with those of the GAM, as shown in [14]. In this paper, this abruptly excited mode is just referred to as 'GAM' in order to avoid confusing the two observed modes, which are the 'EGAM' with the up-chirping frequency and the abruptly excited 'GAM' at approximately 40 kHz.

In addition, several modes also appear at around 97 kHz, 139 kHz and 180 kHz. As shown in figure 4, these frequencies correspond with the addition of 14 kHz to the higher harmonic frequencies of the abruptly excited GAM with a frequency of 41.5 kHz: $2f_d + 14 = 97$, $3f_d + 14 = 138.5$ and $4f_d + 14 = 180$, where f_d (=41.5 kHz) is the frequency of the abruptly excited GAM. The toroidal mode numbers of the GAM and EGAM are zero, and those of the other modes at 14 kHz, 97 kHz, 139 kHz, and 180 kHz are one, as shown

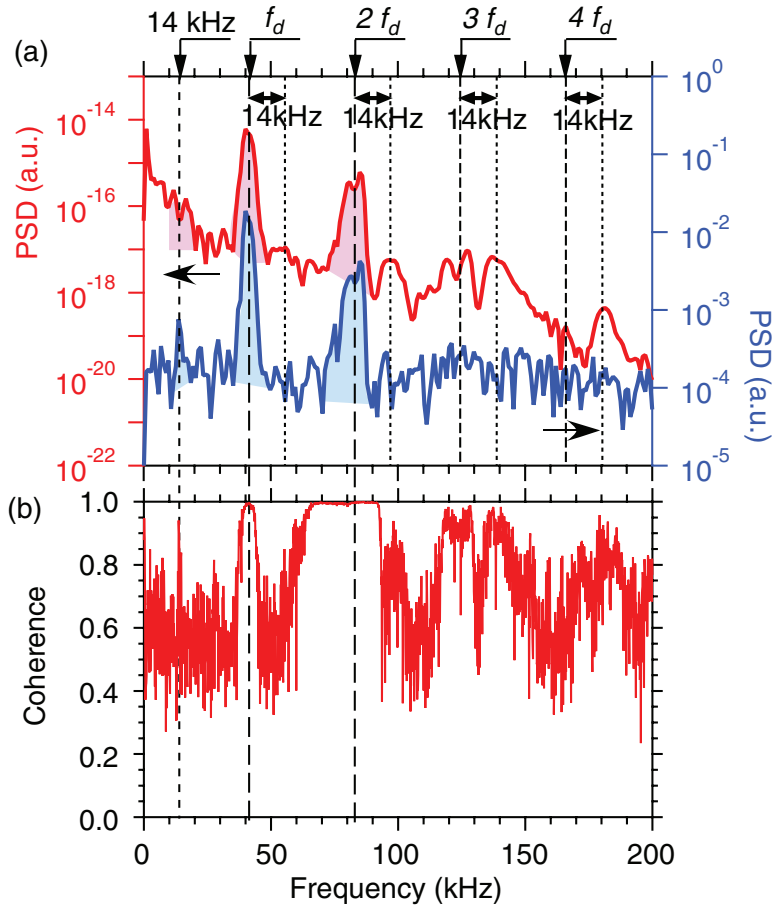

Figure 4. (*a*) The frequency spectra of the magnetic field fluctuation (left-hand side) and the electric potential fluctuation (right-hand side). (*b*) The coherence between the magnetic field fluctuations measured by two Mirnov coils aligned in the toroidal direction.

in figure 5. This relation between the frequencies suggests a coupling between the higher harmonics of the abrupt GAM and a mode with a frequency of 14 kHz. Because the amplitudes of the high-frequency modes (>90 kHz) are more than one order of magnitude less than those of the EGAM and the abruptly excited GAM at 41.5 kHz, their contribution to the abrupt excitation phenomenon can be neglected.

The amplitude of $\widetilde{B}_\mathrm{p}$ associated with the abrupt GAM is typically 5 μT, and this is approximately two times larger than the maximum amplitudes of the EGAM, which is 2 μT. If the abrupt excitation is caused by a simple parametric coupling, the power and the frequency must satisfy the Manley–Rowe relation [36]: $P_1/f_1 = P_2/f_2$, where P and f are the power and the frequency, and the subscript indicate the coupling modes. The observed abrupt GAM and EGAM do not satisfy this relation. Thus, the abrupt excitation is not caused by a simple parametric coupling.

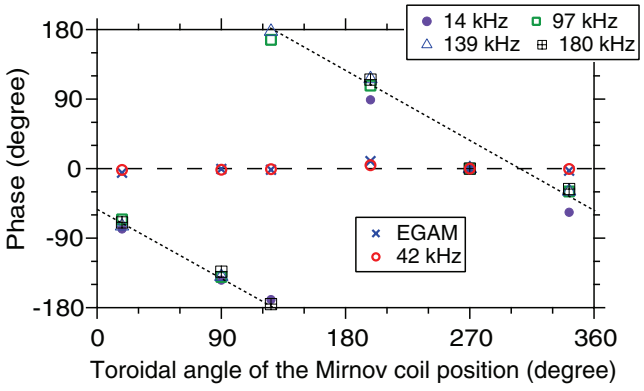

Figure 5. The phase of the magnetic field fluctuations. The horizontal axis is the toroidal angle of the position of the Mirnov coils.

3.2. Nonlinear evolution of the abruptly excited GAM

A nonlinear evolution of the GAM has been observed. Figure 6 shows the temporal evolution of the amplitude of the GAM and its time derivative. The instantaneous growth rate (γ_exp) can be estimated as $\gamma_\mathrm{exp} = \left(\mathrm{d}\left|\widetilde{B}_\mathrm{p}\right|/\mathrm{d}t\right)/\left|\widetilde{B}_\mathrm{p}\right|$, where $\left|\widetilde{B}_\mathrm{p}\right|$ is the amplitude of the mode.

Figures 6(*a*) and (*b*) correspond to a case where the GAM reaches moderate amplitude. After the GAM is triggered, the growth rate decreases monotonically as the amplitude increases. This behavior is common, because the driving source is consumed by the mode excitation. In contrast, in the case in which the GAM is strongly excited, as shown in figures 6(*c*) and (*d*), although the growth rate decreases monotonically for small amplitudes, it increases with an increasing amplitude when the amplitude exceeds a threshold of approximately 2 μT. Figure 7 summarizes the relation between the growth rate and the amplitude in several events under similar experimental conditions, and it indicates the reproducibility of the threshold at approximately 2 μT in this experimental condition. This

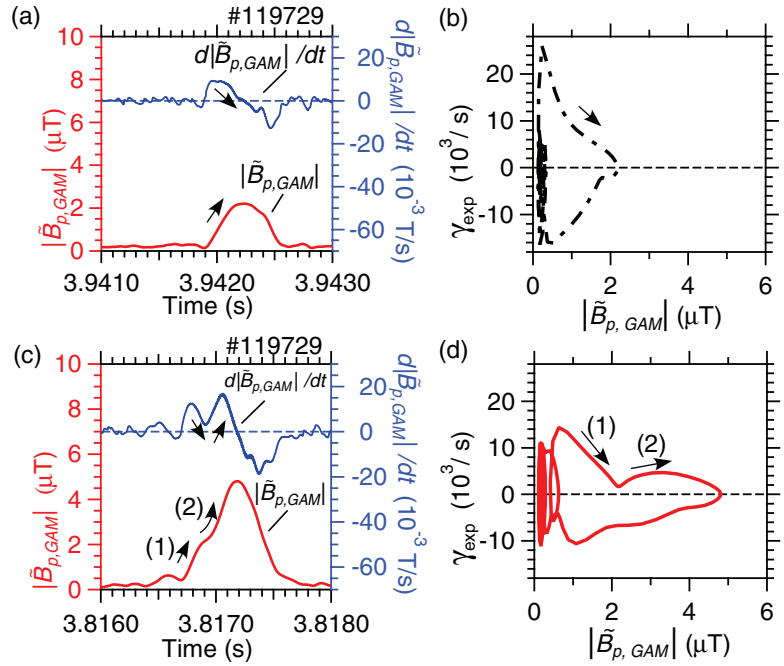

Figure 6. The growth rate of the GAM. (*a*) and (*c*) The typical temporal evolution of the amplitude associated with the GAM ($|\tilde{B}_{p,GAM}|$), and its time derivative. (*b*) and (*d*) The amplitude dependence of the time-dependent growth rate estimated as $\gamma_{exp} = \left(d|\tilde{B}_{p,GAM}|/dt\right)/|\tilde{B}_{p,GAM}|$; (*b*) and (*d*) correspond with the periods of (*a*) and (*c*), respectively.

reacceleration of the growth rate cannot be explained by linear instabilities, as long as the direction of change in the driving source, such as the gradient in the phase space and the pressure gradient, does not vary for a short period. In the timescale of the GAM, the heating power of NBI and ECH is constant and the electron density is almost constant as shown in figure 2. Thus, the reacceleration of the growth rate is an essential nonlinear feature of the mode excitation.

3.3. Phase relation between the abruptly excited GAM and the EGAM

The abruptly excited GAM only appears in the presence of the chirping EGAM. Thus, the GAM is normally stable, and the presence of the EGAM seems to be a necessary condition for the abrupt excitation of the GAM. In order to confirm and characterize the link between the GAM and the EGAM, the phase relation between them has been investigated.

Figure 8 shows the phase difference (δ) between the abruptly excited GAM and the EGAM during the GAM excitation, where the phase difference δ is defined as $\tilde{B}_{GAM} \propto \cos(2\pi f_d t + \delta)$ for the abruptly excited GAM with a frequency of f_d and $\tilde{B}_{EGAM} \propto \cos 2\pi f_2 t$ for the EGAM with a frequency of f_2. In order to show the reproducibility, the phase differences in three events are plotted in figure 8, and the spectrograms including the analyzed events are shown in figures 9(*a*)–(*c*). The phase relation shows a common tendency in all the events. If the GAM was independent from the EGAM, the phase would be random in each event. As the abrupt GAM evolves, the frequency of the EGAM rapidly changes following the second harmonic frequency of the

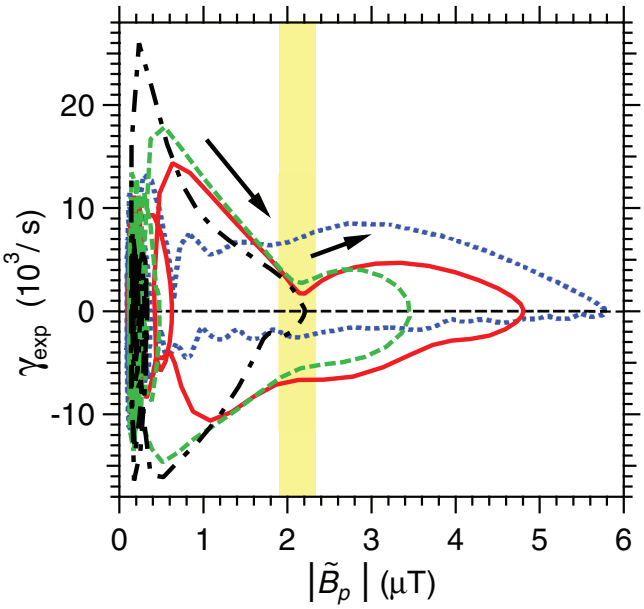

Figure 7. The amplitude dependence of the growth rate in four bursts of the GAM.

GAM, as shown in figures 8(*a*)–(*c*). The specific phase relation and the change in the EGAM frequency during the GAM excitation suggests the mode coupling between the GAM and the EGAM, though a simple parametric coupling cannot explain the abrupt excitation as described in section 3.1. In addition, this coupling cannot be explained by the known driving mechanisms of the GAM, such as the nonlinear coupling of turbulence [37] and the inverse Landau damping by energetic particles [15].

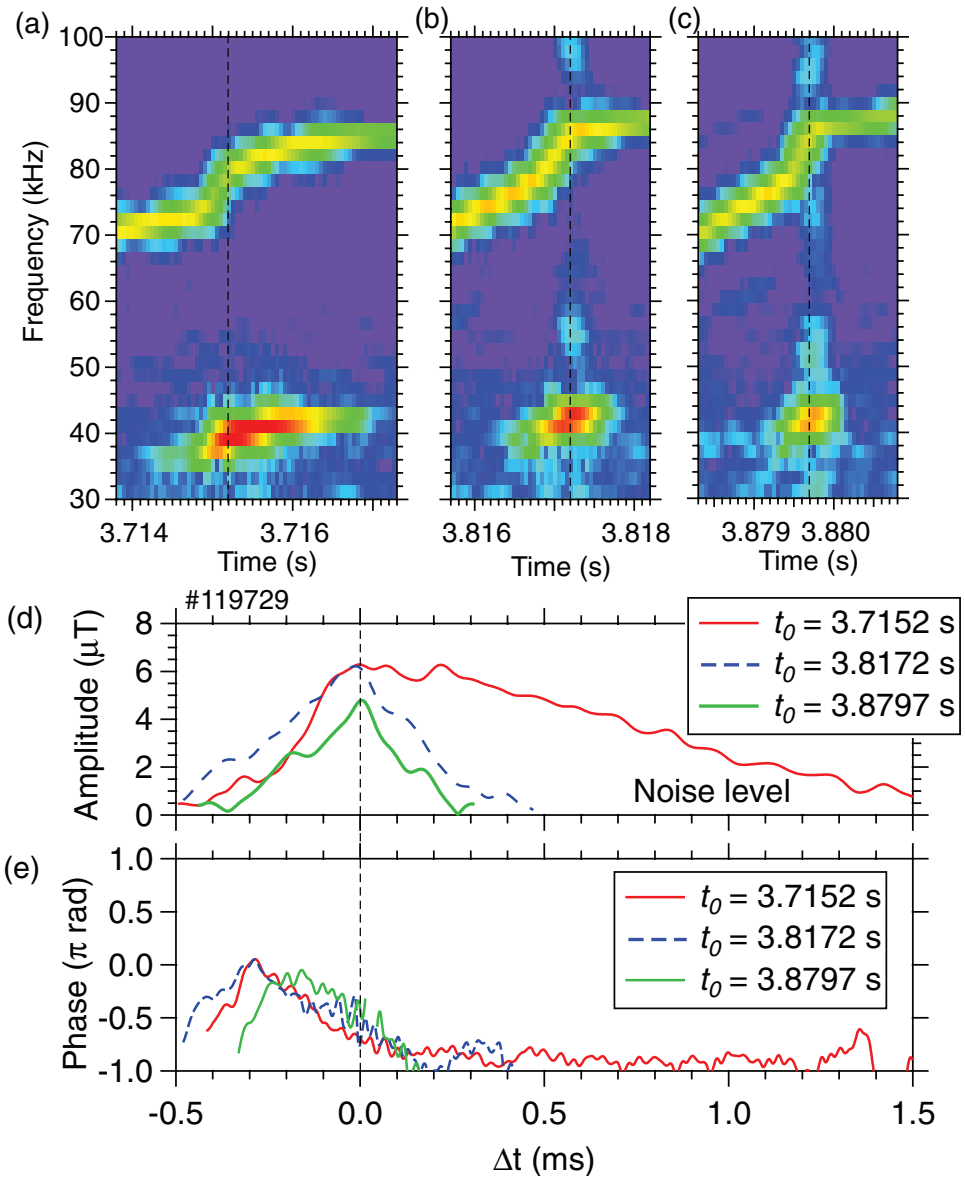

Figure 8. (*a*)–(*c*) An expanded view of the spectrograms of the magnetic field fluctuation. The time window used in FFT is 0.512 ms (256 samples), and the dashed lines indicate the time of the maximum GAM amplitude (t_0). (*d*) The temporal evolution of the amplitude of the abrupt GAMs. The origin of the horizontal axis indicates the time of the maximum GAM amplitude. (*e*) The phase difference (δ) between the GAM and the EGAM, where waveforms of the GAM and the EGAM are expressed as $\widetilde{B}_{\mathrm{GAM}} \propto \cos(2\pi f_d t + \delta)$, and $\widetilde{B}_{\mathrm{EGAM}} \propto \cos 2\pi f_2 t$, respectively.

3.4. Relation between the amplitude of the EGAM and excitation of the GAM

In the previous section, it is revealed that the EGAM is related to the abrupt excitation of the GAM. If the EGAM plays an essential role, the GAM excitation will correlate with the amplitude of the EGAM. Figure 9 shows the relation between the amplitude of the GAM and the amplitude of the EGAM, where the latter amplitude is measured just before the abrupt GAM excitation. This indicates that the GAM is not excited if the amplitude of the EGAM is smaller than 1.2 μT. Thus, there is a threshold in the amplitude of the EGAM for the abrupt excitation of the GAM.

Note that even if the amplitude of the EGAM exceeds the threshold, the GAM is not excited in some cases. This suggests the existence of other parameters determining the abrupt GAM excitation, which will be discussed in the next section.

4. Discussion

The experimental results indicate that the abrupt excitation of the GAM involves a coupling with the EGAM with an up-chirping frequency. However, the coupling cannot be explained by a simple parametric coupling and the known driving mechanisms of the GAM, such as the nonlinear coupling of turbulence and the inverse Landau damping, as described above.

According to the theoretical model proposed in [25–27], the subcritical instability of the GAM can be driven by a

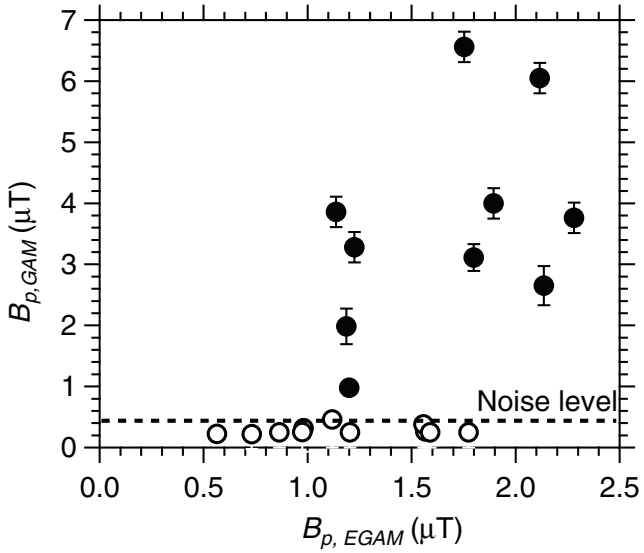

Figure 9. The relation between the amplitude of the EGAM (horizontal axis) and the amplitude of the abruptly excited GAM (vertical axis). In the case in which the abrupt GAM is apparent (filled circles), the amplitude of the EGAM is measured just before the onset of the GAM, and the amplitude of the GAM is its maximum amplitude. In the case in which the presence of the abrupt GAM is unclear (open circles), the amplitude of the EGAM is measured at the same frequency as the other EGAMs, accompanied by an abrupt GAM under similar experimental conditions.

cooperative collaboration of the kinetic nonlinearity, which corresponds with the resonant interactions between the GAM and the energetic particles, and fluid nonlinearity, which corresponds with the nonlinear parametric coupling between the EGAM (mother mode) and the GAM (daughter mode). Thus, the abrupt excitation phenomenon can be interpreted as the subcritical instability of the GAM (daughter mode) triggered by the chirping EGAM (mother mode), and the energy of the instability comes from the EGAM (mother mode) and the energetic particle. The timescale of the GAM excitation, the phase relation and the amplitude relation between the GAM and the EGAM are reproduced by the model as shown in [25]. Recently, another simulation by the MEGA code [35, 38] which is a hybrid simulation code taking into account kinetic energetic particles and an MHD fluid, shows that the coupling between the GAM and the EGAM arises only from a kinetic coupling via energetic particles [39]. Although, at present, the amplitude of the excited GAM is much smaller than that of the EGAM in the simulation, unlike the experimental results [39] indicates that the kinetic coupling induced by the resonant interaction between the EGAM with the second harmonic GAM frequency and energetic particles causes the GAM oscillation with the fundamental GAM frequency. The coupling may become a trigger of the subcritical instability with a large amplitude if a sufficient seed to exceed the threshold for a subcritical instability is given. Thus, neither of the candidate theories contradict the interpretation, in which the observed relation between the GAM and the EGAM indicates that the EGAM triggers the abrupt GAM excitation; however, the coupling mechanism triggering the instability has not been identified yet.

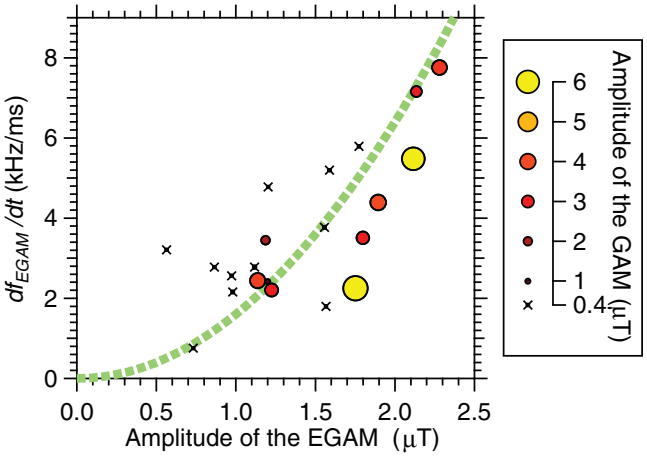

Figure 10. Parameters in which the abrupt GAMs are excited. The horizontal axis is the amplitude of the EGAM, and the vertical axis is the chirping rate of the EGAM. The data is the same as that in figure 9. The size of the markers indicates the amplitude of the excited GAM. The noise level at 0.4 μT. The dotted curve shows $\mathrm{d}f_{\mathrm{EGAM}}/\mathrm{d}t \propto \left|\widetilde{B}_{\mathrm{p,EGAM}}\right|^2$, as an eye guide.

The excitation of the subcritical instability requires a seed with sufficient amplitude and a trigger. The threshold in the amplitude of the GAM (figure 7) can be interpreted as the required amplitude of the seed, and the threshold in the amplitude of the EGAM (figure 9) can be interpreted as corresponding with the threshold in the trigger. Thus, the experimental results indicate that the abrupt excitation phenomenon has the nature of a subcritical instability.

The scattering data in figure 9 can be explained by the theoretical model in [26]. According to the theoretical model, the threshold has been analytically predicted as $D^2 \geqslant \mathrm{d}\theta/\mathrm{d}t$, where D is proportional to the amplitude of the EGAM, and $\mathrm{d}\theta/\mathrm{d}t$ is the chirping rate frequency of the EGAM if the linear growth rate of the GAM is small. Thus, the theory predicts that the excitation condition is determined not only by the magnitude of the EGAM, but also by the frequency chirping rate. In other words, the threshold in the amplitude of the EGAM for the abrupt GAM excitation depends on the frequency chirping rate of the EGAM. Figure 10 provides a summary of the parameters (amplitudes and chirping rate) where the abrupt GAM is excited. Here, the analyzed data is the same as that in figure 9. The excitation boundary seems to agree with the theoretical prediction of the excitation threshold, which is $D^2 \geqslant \mathrm{d}\theta/\mathrm{d}t \propto \mathrm{d}f/\mathrm{d}t$, qualitatively.

The threshold in the trigger (figure 9) and the threshold in the amplitude (figure 7) are the essential features of a subcritical instability, and the theoretical prediction of the parameter dependence of the threshold agrees with the experimental result (figure 10). Therefore, the observed abrupt phenomenon can be interpreted as the excitation of the subcritical instability of the GAM.

5. Summary

Abrupt excitation of a GAM has been found in the LHD, when the frequency of the chirping EGAM approaches twice that of the GAM frequency. The phase relation between the GAM and the

EGAM is common in all excitation events, and it indicates mode coupling between the GAM and the EGAM. However, the relation between the amplitude variations of the abrupt GAM with the lower frequency and the EGAM with the higher frequency does not satisfy the Manley–Rowe relation. Thus, although mode coupling is involved, it does not explain the abrupt excitation.

The observed characteristics of the abrupt excitation of the GAM, such as the phase, the amplitude and timescale of the evolution, can be explained by a theoretical model [25–27], which shows that the subcritical instability of the GAM can be driven by a cooperative collaboration between kinetic nonlinearity and fluid nonlinearity. The observed threshold in amplitude of the GAM for the reacceleration of the growth rate seems to correspond with the threshold in the magnitude of the seed required for the growth of the subcritical instability, and the threshold in the amplitude of the EGAM for the GAM excitation seems to correspond with the threshold in the magnitude of the trigger. Thus, the observed thresholds indicate that the abrupt excitation phenomenon of the GAM with a large amplitude has a subcritical instability nature, and this experiment would be the first demonstration of the presence of subcritical instability in magnetically confined plasmas. Since a subcritical instability is one of the working hypotheses [1] of the onset of abrupt phenomena such as sawtooth oscillation and disruption in laboratory plasmas, as well as solar flares in astro-plasmas, this study identifies an experimental path for exploring the trigger problem of abrupt phenomena.

Acknowledgments

The authors thank Dr H. Wang and Prof Y. Todo of the National Institute for Fusion Science and Dr N. Yokoi of the University of Tokyo for useful discussions, as well as the LHD Technical Group for its support. They are also grateful to Dr K. Hallatschek of the Max-Planck-Institute for Plasma Physics and Dr K. Shinohara of the National Institutes for Quantum and Radiological Science and Technology for their valuable comments. This work was supported by MEXT Japan under the Grant-in-Aid for Scientific Research (A) (no. 15H02155), (C) (no. 24561031, 15K06653), for Challenging Exploratory Research (no. 24656561, 16K13923), for Young Scientists (B) (no. 15K18305), NIFS/NINS under NIFS10ULHH020, and the Collaborative Research Program of the Research Institute for Applied Mechanics, Kyushu University.

References

[1] Itoh S., Itoh K., Zushi H. and Fukuyama A. 1998 *Plasma Phys. Control. Fusion* **40** 879
[2] Bhattacharjee A., Ma Z.W. and Wang X. 2003 *Lecture Notes in Physics 614: Turbulence and Magnetic Fields in Astrophysics* (Berlin: Springer)
[3] Yagi M., Itoh S.-I., Itoh K., Fukuyama A. and Azumi M. 1995 *Phys. Plasma* **2** 4140
[4] Carrera R., Hazeltine R. and Kotschenreuther M. 1986 *Phys. Fluids* **29** 899
[5] O'neil T. 1967 *Phys. Fluids* **10** 1027
[6] Dupree T.H. 1982 *Phys. Fluids* **25** 277
[7] Dupree T.H. 1983 *Phys. Fluids* **26** 2460
[8] Berk H., Breizman B., Candy J., Pekker M. and Petviashvili N. 1999 *Phys. Plasma* **6** 3102
[9] Lesur M., Idomura Y. and Garbet X. 2009 *Phys. Plasma* **16** 092305
[10] Lesur M., Idomura Y., Shinohara K. and Garbet X. 2010 *Phys. Plasma* **17** 122311
[11] Nguyen C. *et al* 2010 *Plasma Phys. Control. Fusion* **52** 124034
[12] Lesur M., Diamond P.H. and Kosuga Y. 2014 *Plasma Phys. Control. Fusion* **56** 075005
[13] Winsor N., Johnson J.L. and Dawson J.M. 1968 *Phys. Fluids* **11** 2448
[14] Ido T. *et al* 2016 *Phys. Rev. Lett.* **116** 015002
[15] Fu G. 2008 *Phys. Rev. Lett.* **101** 185002
[16] Boswell C. *et al* 2006 *Phys. Lett.* A **358** 154
[17] Berk H. *et al* 2006 *Nucl. Fusion* **46** S888
[18] Nazikian R. *et al* 2008 *Phys. Rev. Lett.* **101** 185001
[19] Toi K. *et al* 2010 *Phys. Rev. Lett.* **105** 145003
[20] Ido T. *et al* 2011 *Nucl. Fusion* **51** 073046
[21] Matsunaga G., Kamiya K., Shinohara K., Miyato N. and Kojima A. 2012 *Proc. the 39th EPS Conf. on Plasma Physics (Stockholm, 2–6 July)* p P2.062 (http://ocs.ciemat.es/epsicpp2012pap/pdf/P2.062.pdf)
[22] Lauber P. *et al* 2013 *13th IAEA Technical Meeting on Energetic Particles in Magnetic Confinement Systems (Beijing, China, 17–20 September 2013)* (http://www.phy.pku.edu.cn/fsc//admin/fileadmin/upfile/Lauber.Ph.-D.pdf)
[23] Chen W. *et al* 2013 *Phys. Lett.* A **377** 387
[24] Berk H., Breizman B. and Petviashvili N. 1997 *Phys. Lett.* A **234** 213
[25] Lesur M. *et al* 2016 *Phys. Rev. Lett.* **116** 015003
[26] Itoh K., Itoh S.I., Kosuga Y., Lesur M. and Ido T. 2016 *Plasma Phys. Rep.* **42** 418
[27] Lesur M. *et al* 2016 *Nucl. Fusion* **56** 056009
[28] Iiyoshi A. *et al* 1999 *Nucl. Fusion* **39** 1245
[29] Ido T. *et al* 2006 *Rev. Sci. Instrum.* **77** 10F523
[30] Shimizu A., Ido T., Nishiura M. and Kato S. 2010 *Plasma Fusion Res.* **5** S1015
[31] Osakabe M. *et al* 2006 *Nucl. Fusion* **46** S911
[32] Osakabe M. *et al* 2014 *Proc. of the 25th IAEA Fusion Energy Conf. (St. Petersburg, Russia, 13–18 October 2014)* [Ex/10–3] (www.nifs.ac.jp/report/IAEA2014/EX-10-3_Osakabe.pdf)
[33] Ido T. *et al* 2015 *Nucl. Fusion* **55** 083024
[34] Sugama H. and Watanabe T. 2006 *Phys. Plasma* **13** 012501
[35] Wang H., Todo Y., Ido T. and Osakabe M. 2015 *Phys. Plasma* **22** 092507
[36] Manley J.M. and Rowe H.E. 1956 *Proc. IRE* **44** 904
[37] Diamond P.H., Itoh S.-I., Itoh K. and Hahm T. 2005 *Plasma Phys. Control. Fusion* **47** R35
[38] Todo Y., Berk H. and Breizman B. 2010 *Nucl. Fusion* **50** 084016
[39] Wang H., Todo Y. and Suzuki Y. 2016 *Preprint: 2016 IAEA Fusion Energy Conf. (Kyoto, Japan, 17–22 October 2016)* [TH/P4-11] (https://conferences.iaea.org/indico/event/98/session/22/contribution/565/material/paper/0.pdf)
[40] Hirshman S.P. *et al* 1986 *Comput. Phys. Commun.* **43** 143